Proceedings of the IASS 2024 Symposium
Redefining the Art of Structural Design
August 26-30, 2024, Zurich Switzerland
Philippe Block, Giulia Boller, Catherine DeWolf,
Jacqueline Pauli, Walter Kaufmann (eds.)

Cyclic behavior study of LY160 steel shear panel damper

Ziran XU*, Minger WU, Jiachun CUI[a], Yuxiao WU

* College of Civil Engineering, Tongji University
1239 Siping Road, Shanghai, P.R. China
xunature@126.com

[a] Arcplus Group PLC

Abstract

Low-yield-point steel shear panel damper (LSSPD) can be used as energy dissipation components to enhance the seismic performance of spatial structures. The lower the strength of the steel used in the web plate of LSSPD, the better its ductility and energy dissipation capacity, but the higher the overstrength factor. This paper investigates the seismic performance and overstrength factor of a LSSPD with LY160 web plate through cyclic loading test. A LSSPD with LY160 web plate was designed based on the given initial stiffness and yield load. The initial stiffness, bearing capacity, overstrength factor, ductility, stiffness degradation, and energy dissipation characteristics of the LSSPD were studied. The experimental results showed that the initial stiffness and yield load of the LSSPD were basically consistent with the design values. The equivalent viscous damping ratio exceeded 0.5, and the overstrength factor was 2.6, far exceeding the AISC 341-16 provision of 1.5 for links in eccentrically braced frames. It was recommended to pay attention to the design of adjacent structural members and connections with LSSPD. In addition, the accuracy of the finite element model was verified through comparison of experimental and analytical results, and based on this, the influences of flange thickness and stiffener arrangement on the bearing capacity, energy dissipation, and overstrength factor of LSSPD were analyzed.

Keywords: low-yield-point steel shear panel damper (LSSPD), test study, cyclic behavior, energy dissipation, overstrength

1. Introduction

In the past few decades, dampers have been widely used in spatial structures (e.g. capital indoor stadium, Xiong'an stadium in China) for seismic energy dissipation, providing additional damping, stiffness and bearing capacity (e.g. Housner et al. [1], Xue et al. [2], and Xu et al. [3]). Dampers can be divided into three types: velocity type, displacement type, and hybrid type. Among them, metallic displacement type dampers have advantages such as definite stressing state, stable mechanical performance, and simply fabrication [4].

The mechanisms of metallic displacement type dampers mainly include axial compression type (BRB), bending type (ADAS), and shear type [5]. Once the shear type metallic damper chieves its yield in the early stage, the metallic shear web subjected to uniform in-plane shear force allows the material yield to spread over the entire area, maximizing the dissipation of earthquake input energy.

Metallic displacement dampers can use materials such as mild steel (e.g. Kim et al. [6]), lead, aluminum, shape memory alloy (e.g. Lu et al. [7]) for energy dissipation. Previous studies (e.g. Cui et al. [8], Pan et al. [9]) have shown that low-yield-point steel can enable dampers to enter yield earlier and undergo a wide range of plastic deformation to absorb a large amount of seismic energy. In LSSPD, using low-yield-point steel for the web plate and ordinary steel for other components can fully utilize the

advantages of different types of steel, achieving a unity of good bearing capacity, strong energy dissipation, and excellent economy.

When designing adjacent structural members and damper's connections, it is necessary to consider the damper's overstrength factor, which is the ratio of ultimate bearing capacity to yield load [10]. It is suggested that a value of 1.5 can be taken as the overstrength factor of EBF links in the AISC 341-16. Current studies (e.g. Ji et al. [11], Xu et al. [12]) has shown that the overstrength factors of LSSPD reach 1.9 when using LY225 and is approximately 2.8 for LY160.

Although there have been some experimental and finite element analytical studies on LSSPD, it's still far from enough, especially for dampers using LY160 as the web material. At the same time, different manufacturers of low-yield-point materials, different arrangements of stiffeners, different length ratios of dampers, and different fabrication crafts of dampers can all affect the mechanical properties of LSSPD.

In light of the above, cyclic test study on the LSSPD specimen whose web plate made of LY160 produced by Nanjing Iron & Steel Company were conducted. A brief summary of the specimen and test results were then provided. The skeleton curve, initial stiffness, capacity, overstrength, ductility, degradation of stiffness and energy dissipation capacity were further discussed. Finally, finite element model of the LSSPD were established and verified by the experiment results. The influence of flange thickness and stiffener arrangement on the bearing capacity, energy dissipation performance and overstrength of LSSPD was analyzed based on finite element method.

2. Experimental program

2.1. Test specimen

Through the structural design requirements, the initial stiffness and yield load of LSSPD can be determined. At the same time, the steel grade of the web plate, which usually selected from low-yield-point steels LY225, LY160 and LY100, can be determined due to the ductility requirement. Based on the initial stiffness, yield load and steel grade of web plate, the cross-sectional area and the length of web plate can be calculated by the following two formulas.

$$A_s = \sqrt{3}F_y / \sigma_y \tag{1}$$

$$L = \eta G A_s / (1+\eta) K_0 \tag{2}$$

Where A_s and L are the cross-sectional area and the length of web plate respectively; F_y and K_0 are the the initial stiffness and yield load of LSSPD respectively; σ_y and G are the yield strength and shear modulus of the web steel respectively; η is the ratio of initial bending stiffness to shear stiffness, usually can be set from 4 to 9 in the preliminary design phase, which making $\eta/(1+\eta)$ to be from 0.8 to 0.9.

An appropriate ratio of length to width of web plate is beneficial for its energy dissipation. In the preliminary design phase, the aspect ratio can be set as 1.0. When the aspect ratio is set as 1.0, the thickness of the web plate can be calculated through the ratio of A_s to L. It should be noted that the thickness and height of the web plate need to be adjusted according to the thickness modulus specifications of the steel plate. It should also be noted that the influence of flange on yield load although it is minimal.

To prevent web buckling and improve energy dissipation capacity, stiffeners need to be set up on one side or two sides of web plate generally. Appendix B of Technical specification for steel structure of tall building (JGJ 99-2015) in China provides relevant regulations on the stiffness ratio of stiffeners, but it only applies to the case of four-sided connections, and is not applicable to such dampers connected on both sides. AISC 341-16 provides the principle for the arrangement of stiffeners for links in EBF. When the length ratio of a link is not greater than 1.6 and the rotation requirement is 0.08 rad, the maximum spacing should not exceed the difference between 30 times the thickness of the web plate and one-fifth of the height of the web plate, which is adopted by Code for seismic design of buildings (GB 50011-2010) in China.

The geometric dimensions and details of the LSSPD specimen designed with an initial stiffness requirement of 530kN/mm and a yield load requirement of 435kN are shown in Figure 1, ① is the web plate, made of LY160 steel, ② is the flange plates, made of Q355B steel, ③ is the stiffeners, made of Q235B steel, ④ is the end plates, made of Q355B steel.

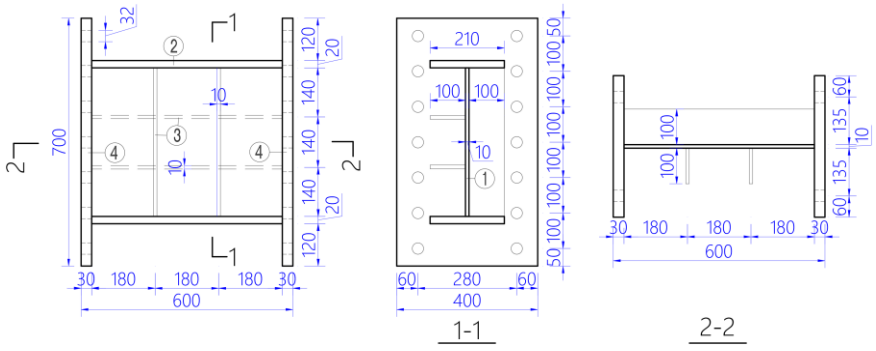

Figure 1: Geometric dimensions and details of the specimen

2.2. Materials

According to the requirements of Steel and steel products – Location and preparation of samples and test pieces for mechanical testing (GB/T 2975-2018) in China, samples were taken from the same batch of steel used in the experiment. Besed on the relevant provisions of Metallic materials – Tensile testing – Part 1: Method of test at room temperature (GB/T 228.1-2021) in China, uniaxial tensile tests were carried out on the samples. The measured results of material properties are shown in Table 1. It can be seen that compared with Q355B and Q235B, low-yield-point steel LY160 has the characteristics of low yield strength, high elongation, and strong plastic deformation ability. In addition, the elastic modulus of LY160 steel obtained through testing three samples is 192.8 GPa.

Table 1: Material properties

Material	Yield strength (MPa)	Ultimate strength (MPa)	Elongation corresponding to fracture (%)
LY160	180	280	54.8
Q235B	283	432	30.2
Q355B	417	566	24.5

2.3. Test setup

The experiment was conducted in the Structural Engineering Laboratory of Zhejiang University. The specimen loading device, which can reflect the actual stress state of specimen, mainly consists of an actuator, an L-shaped loading beam, and a lateral limiting device, as shown in Figure 2(a)(b).

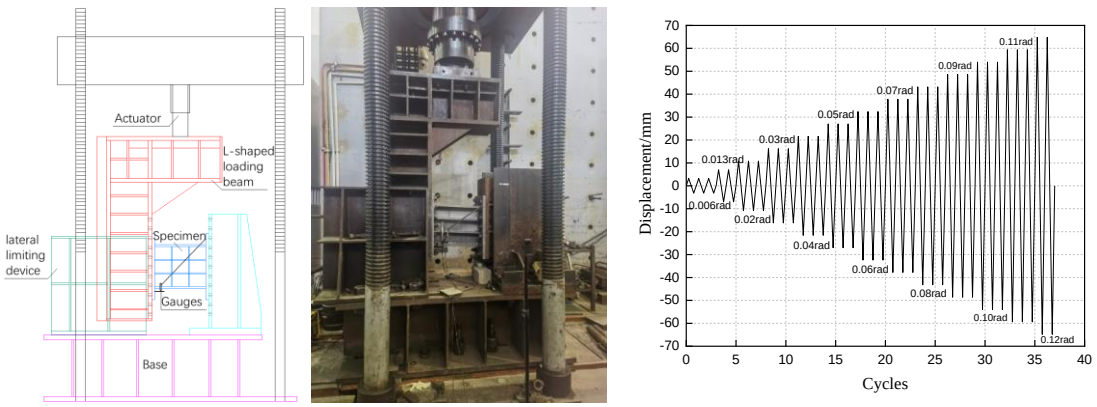

(a) schematic diagram (b) on site photo (c) cyclic loading history

Figure 2: Loading device and loading protocol

2.4. Loading protocol

According to the provisions of the Specification for seismic test of buildings (JGJ/T 101-2015) in China, the loading protocal for quasi-static tests should adopt the load and displacement dual control method, with each level of load being repeated once before yielding and three times after yielding. On the basis of the initial stiffness requirement of 570kN/mm and the yield load requirement of 390kN, the yield displacement calculated is about 0.68mm, which is relatively very small compared to loading and measuring equipment. Therefore, the displacement controlled quasi-static cyclic loading program was used during the entire test. The detailed loading displacement amplitudes and corresponding numbers of cycle are given in Figure 2(c).

2.5. Instrumentation

During the test, the relative vertical displacement of the specimen was used as the control displacement. In order to better measure the deformation of the specimen, two displacement gauges were arranged on both sides of the specimen. The gauges were connected to the end plates through steel rods, as shown in Figure 2(a)(b). The load value of the actuator was collected in real-time through the built-in force sensor.

3. Experimental Results

3.1. Test observation and failure mode

The appearance of the specimen was well until the end of the cyclic loading of 59.4mm(0.11rad). During the first cycle of reciprocating loading of 64.8mm(0.12rad), fractures began to appear on the web plate at the connection with the vertical stiffeners, as shown in Figure 3(a), but no visible out of plane buckling occurred on the web plate. As the loading continued, the web plate tore open along the fractures. Finally, during the second cycle of reciprocating loading of 64.8mm(0.12rad), the bearing capacity of the specimen decreased and could not continue to bear, indicating complete failure of the specimen, as shown in Figure 3(b).

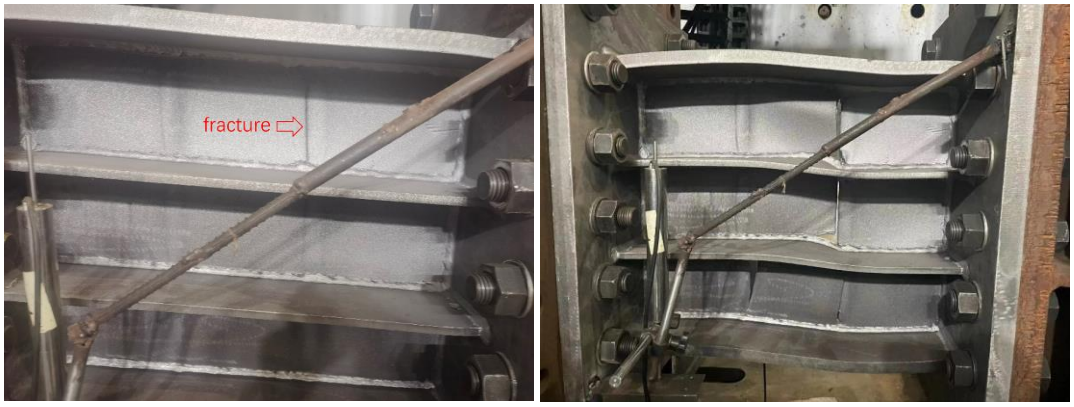

(a) web plate fracture (b) complete failure

Figure 3: Process of specimen failure

3.2. Hysteretic responses

The hysteresis curve of the specimen is shown in Figure 4(a). Due to the instability of displacement measurement starting from 48.6mm(0.09rad) cyclic loading, the hysteresis curve is only given until the end of 43.2mm(0.08rad) cyclic loading. As shown in the Figure 4(a), the hysteresis curve of the specimen is spindle shaped, full and stable, indicating that the specimen has good energy dissipation capacity. During the loading process, as the displacement increases, the bearing capacity of the specimen was increased gradually due to the steel hardening, enhancing energy dissipation of the specimen.

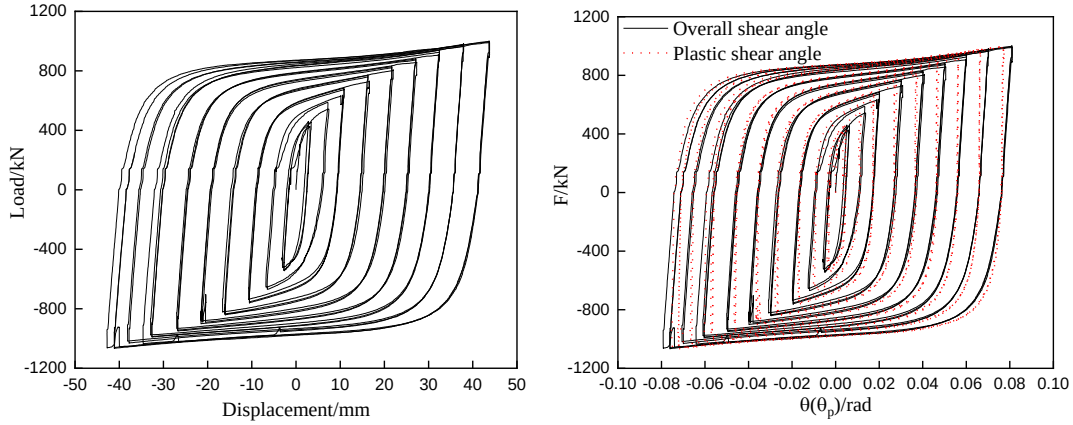

(a) hysteresis curve (b) overall and plastic shear angle

Figure 4: Experimental hysteresis curve and plastic shear angle

4. Discussion of test results

4.1. Skeleton curve

The skeleton curve obtained by connecting the peak value point of each loading level in the load-displacement curve is the outer envelop of the hysteretic curve. Due to the instability of the displacement measured after 43.2mm(0.08rad), theoretical displacement values were used for subsequent displacement data. In addition, since the specimen has entered yield during the first level loading, the yield point data were calculated using the first level hysteresis curve and added to the skeleton curve. The skeleton curve of the specimen is shown in Figure 5(a). The symmetry of the positive and negative directions of the skeleton curve is basically well. For the reasons of the material's hardening effect and positive loading first and then negative, the negative load value at each level of loading is slightly higher than the positive direction.

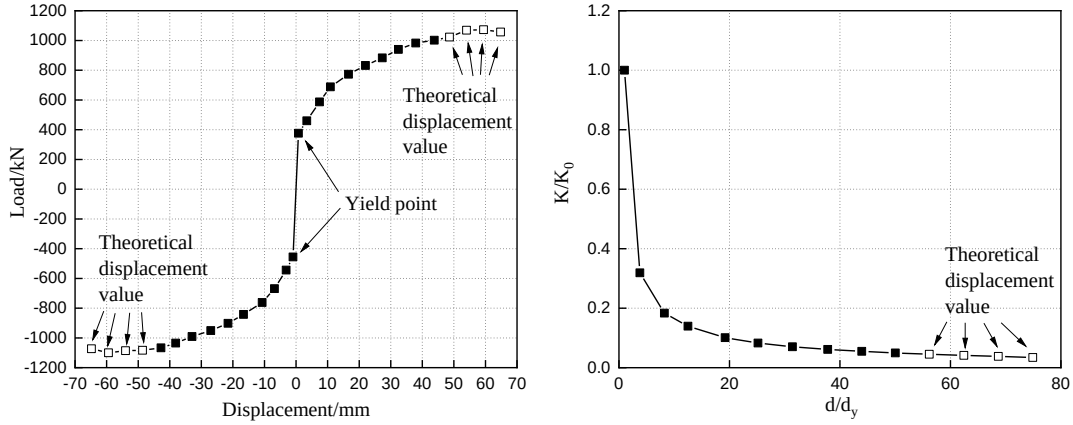

(a) skeleton curve (b) stiffness degration

Figure 5: Experimental skeleton curve and stiffness degration

4.2. Initial stiffness and bearing capacity

According to Standard for building energy dissipation and isolation design (DG/TJ 08-2326-2020) in Shanghai, the initial stiffness, yield load, and ultimate bearing capacity of the specimen can be analyzed from the hysteresis curve of the specimen in Figure 4(a), as shown in Table 2. The testing initial stiffness and yield load in average are 9% and 4% smaller than design values respectively.

Table 2: Mechanical characteristics of the specimen

Loading direction	Design initial stiffness (kN/mm)	Design yield load (kN)	Testing initial stiffness (kN/mm)	Testing yield load (kN)	Ultimate bearing capacity (kN)
Positive	530	435	482	376	1072
Negative	530	435	480	456	1100
Average	530	435	481	416	1086

4.3. Overstrength

The overstrength of LSSPD is very important when designing adjacent structural members and connections. Based on the Table 2, the average positive and negative overstrength factor of the specimen is 2.6, slightly smaller than the results (2.8 in average) in reference (Xu et al. [12]) which using LY160 steel, but far exceeding 1.5 specified in AISC 341-16 which generally used for mild steel and 1.9 suggested in reference (Ji et al. [11]) which using LY225. Therefore, the overstrength is suggested to adopt 2.6 when designing LSSPD using LY160.

4.4. Ductility

Shear panel dampers can characterize their deformation ability through ductility. In combination with the provisions of AISC 341-2016 for the 0.08rad rotation angle limitation of links, the ductility ratio at 0.08rad is given. Besides, the ductility ratio under ultimate deformation is provided. The displacement and ductility ratio of the specimen are shown in Table 3. The plastic shear angle is defined using Eq.3. Moreover, the comparison of the overall shear angle and plastic shear angle for the specimen are conducted, as shown in Figure 4(b).

$$\theta_p = \left(d - F / K_0\right) / L \tag{3}$$

Where d and F represent the displacement and load of the specimen respectively; K_0 is the initial stiffness; L is the length of the specimen.

Table 3: Displacement and ductility ratio of the specimen

Loading direction	Yield displacement (mm)	Displacement at 0.08rad (mm)	Ultimate displacement (mm)	Ultimate shear angle(rad)	Ultimate plastic shear angle(rad)	Ductility ratio at 0.08rad	Ductility ratio
Positive	0.78	43.2	64.8	0.12	0.116	55.4	83.1
Negative	0.95	43.2	64.8	0.12	0.116	45.5	68.2
Average	0.865	43.2	64.8	0.12	0.116	50.4	75.6

4.5. Stiffness degradation

After the LY160 web plate yielded, the stiffness of the specimen was continuously degrated with the increase of loading displacement. Using secant stiffness to describe the stiffness degradation of specimen under reciprocating loads. The stiffness degradation curve with positive and negative average is shown in Figure 5(b). The stiffness degradation ratio is defined as the ratio of the nth level secant stiffness to the initial stiffness, and the vertical and horizontal coordinates are dimensionless. As shown in Figure 5(b), with the displacement increasing, the stiffness degradation ratio decreases fast firstly and then slow.

4.6. Cumulative energy dissipation capacity

The cumulative energy dissipation of the specimen is shown in Figure 6(a), in which the displacement is taken as the mean of positive and negative absolute values. With the increase of displacement, the cumulative energy dissipation of the specimen gradually increases. According to Specification for seismic test of buildings (JGJ/T 101-2015) in China, the calculated equivalent viscous damping ratio ζ_{eq} of the specimen is shown in Figure 6(b). With the increase of displacement, ζ_{eq} of the specimen gradually increases and tends to stabilize, exceeding 0.5 and reaching 0.516, indicating a strong energy dissipation capacity of the specimen.

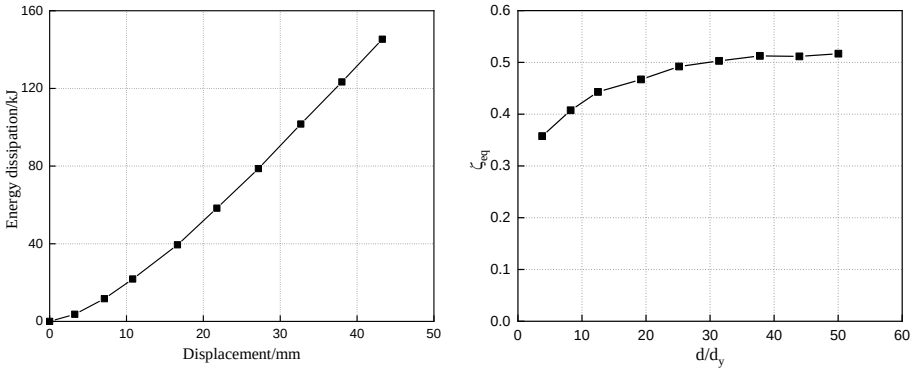

(a) cumulative energy dissipation (b) equivalent viscous damping ratio

Figure 6: Experimental cumulative energy dissipation and equivalent viscous damping ratio

5. Finite element analysis

5.1. Finite element model

The FEM model of the test specimen was established using the finite element package ABAQUS. All components were modeled with the 4-node reduced integral element S4R with the mesh size of 10mm, which was verified for mesh sensitivity. One end of the FEM model was fixed, and the other end was subjected to up and down reciprocating displacement. The loading protocol is consistent with the test specimen. The kinematic-isotropic combined hardening model, whose parameters were obtained from coupon test results and reference [13], was applied for LY160, while conventional structural steels were simulated by the kinematic hardening cyclic plastic constitutive model based on coupon test results.

5.2. Comparision with the experimental result

The comparisons of hysteresis curves, skeleton curves, stiffness degradation curves, culmulative energy dissipation curves, and equivalent viscous damping ratios between test and FEM are shown in Figure 7. It can be seen that the FEM results are in good agreement with the experimental results, indicating that the FEM model established in this paper can accurately reflect the hysteresis characteristic of LSSPD.

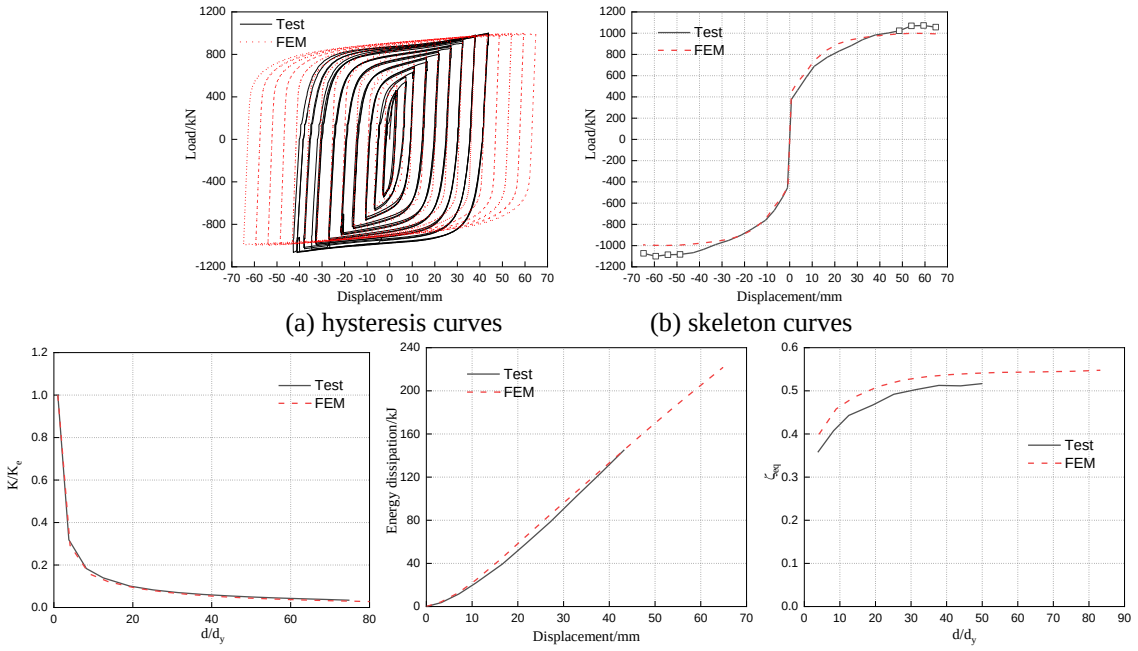

(a) hysteresis curves (b) skeleton curves

(c) stiffness degration (d) cumulative energy dissipation (e) equivalent viscous damping ratio

Figure 7: Comparison of results between FEM and Test

5.3. Equivalent plastic strain

In order to further investigate the plastic characteristics of LSSPD, Figure 8 shows the equivalent plastic strain (PEEQ) of FEM model, which can be used to reflect the plastic cumulative damage of LSSPD. It can be seen that LY160 web plate have entered plasticity entirely, with the maximum PEEQ of 8.58, indicating that the web plate had dissipated a large amount of energy through plastic deformation. In addition, it can be seen that the maximum PEEQ at both ends of the flange plates and vertical stiffeners reached 4.13, indicating that it is necessary to pay attention to the welding quality and welding stress effect of the above areas during LSSPD manufacture.

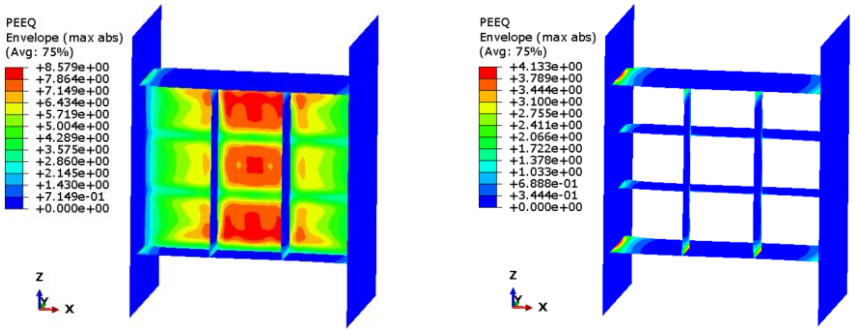

(a) whole model (b) without web plate

Figure 8: PEEQ of FEM model

5.4. Parameter analysis

Through changing the flange thickness, taking 20mm, 15mm, 10mm, and 5mm respectively, the influence of flange thickness on the bearing capacity, energy dissipation and overstrength factor of LSSPD was studied. The comparisons of the primary analysis results are shown in Figure 9. As the thickness of the flange decreases, the yield load remains almost unchange, while the post-yield bearing capacity and cumulative energy dissipation slightly decrease. However, when the thickness of the flange decreases to 5mm, the post-yield bearing capacity and cumulative energy dissipation shows significant degradation, because the flange cannot provide effective constraints on the web. The length ratios of different LSSPD numerical models are listed in Table 4, and the values in parentheses are calculated based on the ultimate strength of the web material. According to AISC341-16, the length ratio can be 1.5 when the rotational demand is not greater than 0.08 rad. As the thickness of the flange decreases, the length ratio of LSSPD gradually increases, leading to a decrease in its rotational capacity and premature degradation of its bearing capacity and cumulative energy dissipation. Therefore, when LY160 is used as the web material for LSSPD and the maximum rotational demand exceeds 0.1 rad, the length ratio is suggested to not be greater than 1.0. When calculating the length ratio, it is advisable to use the effective flange width, while considering the overstrength effect of the web material. As listed in Table 4, when the flange thickness decreases, the overstrength factor gradually decreases, with a decrease of less than 7% within the reasonable design range.

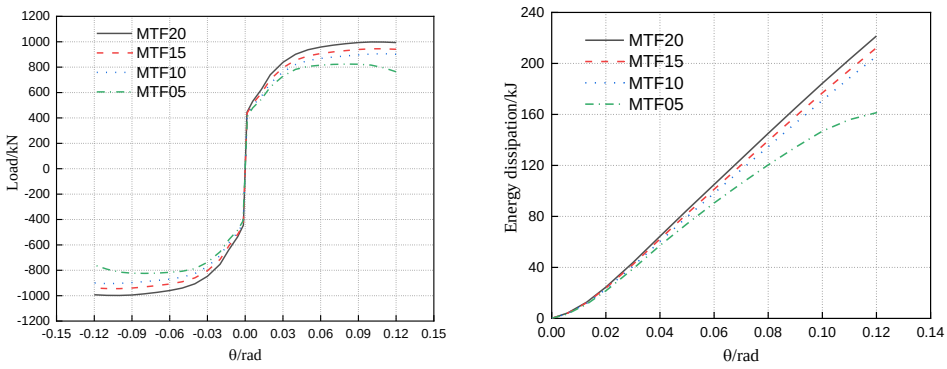

(a) skeleton curve (b) cumulative energy dissipation

Figure 9: Comparison of FEM results on flange plate thickness

Table 4: Length ratios and overstrength factors of different LSSPD numerical models

	MTF20	MTF15	MTF10	MTF05
Nomimal flange width	210mm	210mm	210mm	210mm
Length ratio	0.28(0.41)	0.36(0.53)	0.51(0.73)	0.87(1.15)
Effiective flange width	210mm	210mm	150mm	80mm
Length ratio	0.28(0.41)	0.36(0.53)	0.67(0.92)	1.51(1.80)
Overstrength factor	2.24	2.16	2.10	——

The comparisons of the skeleton curve and cumulative energy dissipation of LSSPD with different stiffener arrangements are shown in Figure 10. "M2V2H" in Figure 10 means model with two vertical stiffeners on one side and two horizontal stiffeners on the other side, and so on. Regardless of whether horizontal stiffeners are arranged or not, both the height to thickness ratio of the web plate and the spacing between vertical stiffeners meet provisions of AISC 341-16. As shown in Figure 10, when the angle exceeds 0.08rad, the post-yield bearing capacity and cumulative energy dissipation of M2V1H and M2V0H show a significant decrease. Therefore, when the rotation requirement exceeds 0.08 rad, the arrangement of stiffeners should be stricter than the provisions of AISC 341-16. Although it can be observed that the skeleton curve and cumulative energy dissipation of M2V2H are similar to those of M2V2V, it should be noted that the mixed arrangement of vertical and horizontal stiffeners can reduce the adverse effects of welding stress on the local area of the web plate to some extent. The overstrength factors of M2V2H and M2V2V are 2.24 and 2.27 respectively, with a difference of about 1%, indicating that the effect of arrangement of stiffeners on overstrength factor of LSSPD can be neglected.

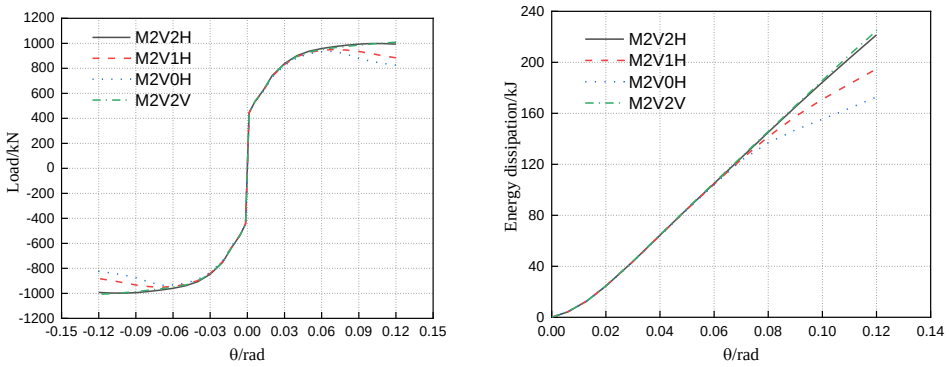

(a) skeleton curve (b) cumulative energy dissipation

Figure 10: Comparison of FEM results on stiffeners

6. Conclusions

This study conducted cyclic loading test on a LY160 steel shear panel damper, whose mechanical and seismic properties such as bearing capacity, initial stiffness, ductility, stiffness degradation, and cumulative energy dissipation were given and discussed. Then finite element analysis and comparison were conducted. Furthermore, the influences of flange thickness and stiffener arrangement on the seismic performance of LSSPD were studied through parameter analysis. Based on the experimental results and finite element analysis results, the main conclusions obtained are as follows:

(1) The hysteresis curve of the LSSPD specimen formed into spindle shape, with ductility ratio exceeding 50 and equivalent viscous damping ratio exceeding 0.5, indicating strong deformation ability and good energy dissipation capacity. The energy dissipation was mainly generated by the plastic deformation of the LY160 web plate, while the vast proportion of other components remained elastic, which was consistent with the design expectations and verified by FEM analysis results.

(2) The initial stiffness and yield load of the specimen were similar to the design values, with a overstrength factor of 2.6, far exceeding 1.5 which the AISC 341-16 set for EBF links. So it is recommended to pay attention to overstrength factor in the design of adjacent structural members and connections of LSSPD using LY160.

(3) The fracture initiated at the connection between the shear web and the vertical stiffeners. In order to dissipate more earthquake input energy by LY160 web plate, better anti-buckling structures or processing techniques need to be proposed to delay the fracture of LY160 web plate.

(4) The FEM results were in good agreement with the experimental results. When LY160 is used as the web material and the maximum rotational demand exceeds 0.1 rad, the length ratio of LSSPD is suggested not be greater than 1.0. It is advisable to use the effective flange width to calculate length ratio and consider the overstrength effect of the web material. Moreover, the arrangement of stiffeners should be stricter than the provisions of AISC 341-16 when the rotation requirement exceeds 0.08 rad. The mixed arrangement of vertical and horizontal stiffeners can achieve a good anti-buckling effect on the web plate. Within a reasonable design range, the influence of flange thickness on the overstrength factor is less than 7%, while the influence of stiffener arrangement on the overstrength factor can be ignored.

Acknowledgements

The authors greatly appreciate the financail supports from Shanghai Science and Technology Plan projects (23DZ1202304).

References

[1] G. W. Housner, L. A. Bergman, T. K. Caughey et al, "Structural control: Past, present, and future," *ASCE Journal of Engineering Mechanics*, vol. 123, no. 9, pp. 897-971, 1997.

[2] S. Xue, Y. Cai, X. Li et al, "The present situation on application of passive control technology in long-span spatial structures," *World Earthquake Engineering*, vol. 25, no. 3, pp. 25-33, 2009. (in Chinese)

[3] X. Xu, F. Gao, W. Ye et al, "Structural design on the stadium of Xiong'an sport center," *Building Structure*, vol. 53, no. 1, pp. 54-58&114, 2023. (in Chinese)

[4] M. Nakashima, S. Iwai, M. Iwata et al, "Energy dissipation behaviour of shear panels made of low yield steel," *Earthquake Engineering and Structural Dynamics*, vol. 23, pp. 1299-1313, 1994.

[5] M. D. Symans, F. A. Charney, A. S. Whittaker et al, "Energy dissipation systems for seismic applications: Current practice and recent developments," *Journal of Structral Engineering*, vol. 134, pp. 3-21, 2008.

[6] J. Kim, T.S. Eom, T.S. Kim, et al, "Structural performance of H-type shear panel damper made of hot-rolled mild steel," *Journal of Constructional Steel Research*, vol. 211, 108134, 2023.

[7] Y. Lu, J. Huang, Q. Han et al, "Hysteretic behavior of a shape memory alloy-friction damper and seismic performance assessment of cable supported structures and reticulated shells," *Smart Materials and Structures*, vol. 29, no. 11, 115003, 2020.

[8] J. Cui, J. Xu, Z. Xu et al, "Cyclic behavior study of high load-bearing capacity steel plate shear wall," *Journal of Constructional Steel Research*, vol.172, 106178, 2020.

[9] Y. Pan, H. Gao, H. Zeng et al, "Study on energy dissipation performance of low-yield-point steel shear panel dampers," *Journal of Constructional Steel Research*, vol. 213, 108351, 2024.

[10] P. Dusicka, A. M. Itani, and I. G. Buckle, "Cyclic behavior of shear links of various grades of plate steel," *Journal of Structural Engineering*, vol. 136, pp. 370-378, 2010.

[11] X. Ji, Y. Wang, Q. Ma et al, "Cyclic behavior of very short steel shear links," *ASCE Journal of Structural Engineering*, vol. 142, no. 2, 04015114, 2016.

[12] L. Xu, X. Nie, J. Fan, "Cyclic behaviour of low-yield-point steel shear panel dampers," *Engineering Structures*, vol. 126, pp. 391-404, 2016.

[13] M. Wang, F. Qian, W. Yang, "Constitutive behavior of low yield point steel LYP160," *Journal of Building Structures*, vol. 38, no. 2, pp. 55-62, 2017.(in Chinese)